

Manipulating Core-Excitations in Molecules by X-ray Cavities

Bing Gu,^{1,*} Artur Nenov,^{2,*} Francesco Segatta,² Marco Garavelli,^{2,†} and Shaul Mukamel^{1,‡}

¹*Department of Chemistry and Department of Physics and Astronomy, University of California, Irvine, 92697, USA*

²*Dipartimento di Chimica Industriale "Toso Montanari",*

Università degli studi di Bologna, Viale del Risorgimento 4, 40136 Bologna, Italy.

Core-excitations on different atoms are highly localized and therefore decoupled. By placing molecules in an X-ray cavity the core-transitions become coupled via the exchange of cavity photons and form delocalized hybrid light-matter excitations known as core-polaritons. We demonstrate these effects for the two inequivalent carbon atoms in 1,1-difluoroethylene. Polariton signatures in the X-ray absorption, two-photon absorption, and multidimensional four-wave mixing, signals are predicted.

Hybrid light-matter states between the material polarization and cavity photon modes, known as polaritons, are created when the light-matter coupling strength g is larger than the decay rate of the cavity mode and the decoherence rate of the molecular transition (the strong coupling regime). When the cavity mode is in the vacuum state, the effective coupling strength for an assembly of N identical molecules is $\kappa = g\sqrt{N}\mu$, $g \equiv \sqrt{\frac{\hbar\omega_c}{2\varepsilon_0V_c}}$, where ε_0 is the electric permittivity of vacuum, ω_c the cavity frequency, μ the transition dipole moment, and V_c is the cavity mode volume [1]. The \sqrt{N} factor is responsible for cooperative superradiance [2, 3]. Cavity polaritons in the visible and infrared regime have long been studied in atoms and were recently experimentally reported in molecules [4–11]. Molecular electronic and vibrational polaritons have been experimentally shown to alter the electronic, optical, and chemical properties of molecules including photoisomerization, electronic energy transfer, electron transfer, and ground-state reaction rates [9]. These findings had triggered intensive theoretical investigations [3, 6, 12–30].

Thin-film optical cavities in the hard X-ray regime have been recently employed in the study of collective Mössbauer signals of ⁵⁷Fe nuclei (14.4 keV) [31–33] and tantalum L-edge X-ray spectra (9881 eV) [34]. A ~ 41 eV effective light-molecule coupling strength for low-finesse X-ray cavities has been reported [34]. X-ray cavities in the soft X-ray regime can be formed by alternating nanometer layers of materials with different indices of refraction, and are on the horizon. For high-reflectivity mirrors, the cavity photon modes satisfy $(n + \frac{1}{2})\lambda_n = L$, where L is the cavity length and λ_n is the wavelength of the cavity mode. For carbon K-edge (~ 300 eV), it corresponds to $L \sim 10$ nm.

Here we study molecular polariton effects in the X-ray regime whereby a high-finesse X-ray cavity mode couples to molecular core-excitations. We demonstrate that localized excitations from inequivalent carbon core-orbitals in 1,1-difluoroethylene can be coupled by the exchange of

an X-ray cavity photon, leading to hybrid core-excitation with X-ray cavity photon modes. Rich exciton-polariton physics has been observed in the optical regime. This includes long-range transport [35, 36], enhanced optical nonlinearity, modified chemical reactions, polariton lasers, optical transistors, and phase transitions [9]. Our study suggests that similar phenomena may be expected for core-polaritons in the X-ray regime. X-ray cavities enable long-range transport of core-excitations or core-holes despite their highly localized nature as long as the light-matter coupling strength is stronger than their decay rates [35, 36]. We predict signatures of core-polaritons in the X-ray absorption spectrum, in two-dimensional (2D) X-ray four-wave mixing signals: photon echo and double quantum coherence, and in the two-photon absorption. Time-domain 2D spectroscopic techniques provide a versatile tool for exploring the optical properties of matter [37, 38]. Multidimensional X-ray spectroscopy enabled by X-ray lasers [39] can [40–42] capture electron dynamics on the attosecond (as) time scale, and can reveal the correlations among core-excitations.

We consider a system of N molecules coupled to a single X-ray cavity mode described by the Hamiltonian $H = H_M + H_{CM} + H_{LM}(t) + H_C$ where the n -th molecular Hamiltonian $H_M^{(n)} = \sum_{j \in \{g,e,f\}} \hbar\omega_j |j^{(n)}\rangle \langle j^{(n)}|$, the cavity Hamiltonian $H_C = \hbar\omega_c a^\dagger a$, and the cavity-molecule coupling $H_{CM} = \sum_{n=1}^N -\boldsymbol{\mu}^{(n)} \cdot \hat{\mathbf{E}}(\mathbf{r}_n, t)$. Here $\boldsymbol{\mu}^{(n)}$ is the transition dipole moment and $\hat{\mathbf{E}}(\mathbf{r}) = i\sqrt{\frac{\hbar\omega_c}{2\varepsilon_0V_c}} \mathbf{e}_c a e^{i\mathbf{k}_c \cdot \mathbf{r}} + \text{H.c.}$ is the electric field operator where a (a^\dagger) is the boson annihilation (creation) operator for the cavity mode, $\mathbf{k}_c, \mathbf{e}_c$ are the cavity mode wave vector and polarization, respectively, H.c. stands for the Hermitian conjugate. We focus on the single- and double-core carbon K-edge excited states, labeled e and f , respectively. Double-core excitations of the same carbon atom are excluded, as they are blue-shifted by tens of eV with respect to doubly core-excited states on different atoms [43]. This shift can be attributed to the reduced electron shielding caused by the first core-excitation which shifts a second core-excitation from the same atom to the blue. The electric-dipole coupling $H_{LM}(t)$ describes the interaction of the molecules with external laser pulses.

For $N > 1$ and $|\mathbf{k}_c \cdot (\mathbf{r}_n - \mathbf{r}_m)| \ll 1$, it is con-

* These authors contributed equally to this work.

† marco.garavelli@unibo.it

‡ smukamel@uci.edu

venient to introduce the collective core-exciton states $|E_{\alpha k}\rangle = \frac{1}{\sqrt{N}} \sum_{n=1}^N e^{ikn} |g^{(1)} \dots g^{(n-1)} e_{\alpha}^{(n)} g^{(n+1)} \dots\rangle$ describing a superposition of a single excitation shared by all molecules and similarly $|F_{\mu k}\rangle$, where $k = 2\pi j/N$, $j = 0, \dots, N-1$. Here α and μ run over the singly and doubly excited states, respectively. Up to double excitations, the cavity-molecule coupling can be represented by (see Sec. S1 for details)

$$H_{\text{CM}} = \sum_{\alpha} \sqrt{N} \kappa_{e_{\alpha}g} |E_{\alpha 0}\rangle \langle G| a + \sum_k \sum_{\mu, \alpha} \kappa_{f_{\mu}e_{\alpha}} |F_{\mu k}\rangle \langle E_{\alpha k}| a + \sum_{n \neq m} \sum_{\alpha, \gamma} \kappa_{e_{\alpha}g} |e_{\alpha}^{(n)} e_{\beta}^{(m)}\rangle \langle e_{\beta}^{(m)}| a + \text{H.c.} \quad (1)$$

where $|G\rangle = |g^{(1)} \dots g^{(N)}\rangle$. Equation (1) implies that the transition from the ground-state to the delocalized core-exciton states $|E_{\alpha 0}\rangle$ is enhanced by \sqrt{N} whereas the coupling between excited states $|E_{\alpha k}\rangle$ and $|F_{\beta k}\rangle$ does not show such cooperativity [3]. The bright state $|E_{\alpha 0}\rangle$ is invariant under exchange of any two molecules. The dark states $|E_{\alpha k}\rangle$, $k \neq 0$ do not contribute to the absorption spectrum. Nevertheless, the transitions between the single-polariton and the dark biexciton states are coupled to the cavity mode by the $|F_{\beta k}\rangle \langle E_{\alpha k}| a + \text{H.c.}$ term even for $k \neq 0$. Note that bright polariton states can relax to the dark states due to e.g. vibronic couplings, disorder, and cavity loss [3, 44]. The third term in Eq. (1) represents the coupling between the singly and doubly core-excited states from different molecules (Sec. S1).

Figure 1 depicts the ground state structure of 1,1-difluoroethylene optimized at the Møller-Plesset second-order perturbation level, and compares the simulated and experimental X-ray absorption near edge structure (XANES) in the [280, 296] eV spectral range. This molecule has two inequivalent carbon atoms with bound pre-edge transitions separated by a few eV. The electronic structure computations are detailed in Sec. S2, and the spectroscopic simulations in Sec. S3 [45]. The simulated XANES spectrum (without any shift) is in excellent agreement with experiment in the [280, 296] eV spectral range. The spectrum has four main features. The 285.6 eV and 289.5 eV peaks are associated with excitations from the $1s$ core orbitals of the carbon atoms in the CH_2 and CF_2 groups to the anti-bonding π^* orbital, respectively. A broader peak at 293 eV, arises from a pair of close lying transitions from CH_2 to Rydberg (Ry) orbitals. Finally, we find a red shoulder to the 289.5 eV band at 288.4 eV, associated with a transition from CH_2 to a σ^* anti-bonding orbital localized in the CH_2 fragment. The ~ 4 eV energy splitting between the $\text{CH}_2 \rightarrow \pi^*$ and $\text{CF}_2 \rightarrow \pi^*$ peaks shows that functionalization with electron withdrawing groups such as fluorine makes core-excitations more energy-costly, thus inducing a few eV blue-shift. The K-edge spectrum is dominated by the core-excitations of CH_2 .

In the X-ray cavity, the core-excitations are modified by coupling to the cavity mode. Figure 2 (top) illus-

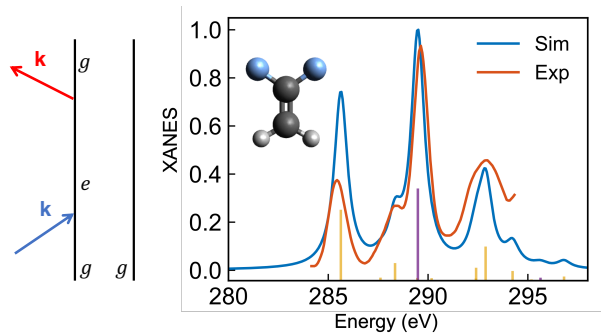


FIG. 1. The XANES spectrum of 1,1-difluoroethylene and the corresponding (left) Feynman diagram. \mathbf{k} denotes the incoming pulse wave vector. (right) The transitions involving the carbon K-edge in CH_2 (CF_2) are represented by yellow (purple) sticks. The agreement with experiment [46] are excellent.

trates the XANES of core-polaritons at cavity frequencies $\omega_c = 290$ eV close to the $\text{CF}_2 \rightarrow \pi^*$ excitation for varying coupling strength. At $g\sqrt{N} = 2.45$ eV/Debye (eV/D), we observe a vacuum Rabi splitting of two polariton peaks. The transition dipole is in the order of 0.1 D. The Rabi splitting is increased with the coupling strength, and the lower polariton further mixes with CH_2 excitations leading to enhancement and redshift of the $\text{CH}_2 \rightarrow \pi^*$ transition.

To unveil the polaritonic nature of the core-excitations in the X-ray cavity, we have decomposed each polariton state into the CH_2 , CF_2 and the cavity photon components. These are depicted in the lower panels in Fig. 2. Since the core-excitations localized at CH_2 and CF_2 are decoupled, each excitation is either purely CH_2 or CF_2 type. To decompose the polariton states, we introduce the projection operators $\mathcal{P}_{\sigma} = \sum_{\alpha \in \sigma} |e_{\alpha}\rangle \langle e_{\alpha}|$ where $\sigma = \{\text{cavity photon}, \text{CH}_2, \text{CF}_2\}$. The σ -component in a polariton state $|\Psi\rangle$ is computed as $P^{\sigma} = \langle \Psi | \mathcal{P}_{\sigma} | \Psi \rangle$. As shown in Fig. 2, without cavity ($g = 0$), all excitations are either purely CH_2 (yellow) or CF_2 (purple) type. As the coupling is turned on, the two ~ 290 eV excitation contain mixed CF_2 and photon (brown) character, reflecting a hybridization of the $\text{CF}_2 \rightarrow \pi^*$ and the cavity photon, resembling the polariton states in a Jaynes-Cummings model. As g increases, the polariton states further mix with CH_2 -excitations, leading to delocalized core-excitations from both CH_2 and CF_2 . The delocalization can be clearly observed in the decomposition of the polariton states ~ 290 eV. These delocalized excitations involving both C atoms arise from an effective coupling between their core excitations induced by exchanging cavity photons even when the cavity is in the vacuum state. When the cavity frequency is detuned far from any resonance in the bare XANES $\omega_c = 288$ eV (bottom row of Fig. 2), no substantial changes in the spectrum are observed at $g = 2.45$ eV/D. Nevertheless, as g gets stronger, we observe similar delocalized core-excitations involving both CH_2 and CF_2 at e.g. 290 eV.

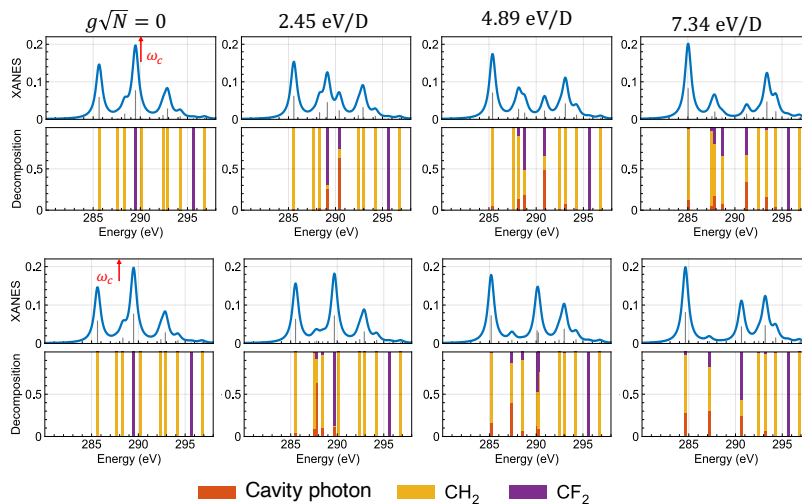


FIG. 2. XANES of 1,1-difluoroethylene in an X-ray cavity for varying coupling strength. Lower panels show the decomposition of each polariton state into CH_2 , CF_2 and photon components. The top row is for cavity frequency $\omega_c = 290$ eV close to a specific transition, and the bottom row for cavity frequency $\omega_c = 288$ eV detuned from the main core-transitions. The dependence on N is solely through the (collective) coupling strength $g\sqrt{N}$.

For nonlinear X-ray signals, we focus on the single-molecule $N = 1$ strong coupling case. Single-molecule strong coupling requires a substantial field enhancement, and its realization may benefit from an ensemble of auxiliary emitters [47]. The signals for large N can depend on many collective dark states that are neglected here. Doubly core-excited dark states $|e_\alpha^{(n)} e_\beta^{(m)}\rangle$ in different molecules also need to be taken into account. Such states do not show up in bare nonlinear spectroscopy due to destructive interference [48, 49]. The cavity mode mediates an effective coupling even for otherwise non-interacting molecules, and the two-core-exciton states from different molecules will influence the bipolariton manifold. Below g, e, f label the ground, single-polariton, two-polariton states, respectively, see Fig. 3 for the level scheme.

We have computed time-domain heterodyne-detected

The 2D PE signals are displayed in Fig. 3. There are three contributions to the spectra: stimulated emission (SE) and ground-state bleaching (GSB) (the first two diagrams in Fig. S1), and the excited state absorption (ESA, the last diagram in Fig. S1). The four XANES features discussed earlier give rise to four traces along Ω_1 (i.e., CH_2 excitations at 285.6 eV, 288.4 eV and 293.0 eV and CF_2 excitations at 289.5 eV) with a characteristic cross peak pattern, that reflects the correlation between various transitions. The cross peaks result from the fact that they share a common ground state, and that the core excitations are both anharmonic $\omega_{fe} \neq \omega_{eg}$ and coupled $\omega_{fg} \neq \omega_{eg} + \omega_{e'g}$. ESA signals related to double core-excitations from the same carbon atom do not cancel the

2D X-ray four-wave mixing signals of core-polaritons. These allow us to track the time-evolution of the polariton states and reveal correlations between transitions. The total electric field is decomposed into three pulses $E(t) = E_3(t) + E_2(t + T_2) + E_1(t + T_1 + T_2) + \text{c.c.}$ where T_j is the time-delay between the j -th and $j + 1$ -th pulse. Labeling the wave vectors of the incoming pulses as \mathbf{k}_j , we first discuss photon echo (PE) signal at $-\mathbf{k}_1 + \mathbf{k}_2 + \mathbf{k}_3$.

The 2D PE spectra are sketched by the Liouville space pathways represented by Feynman diagrams [37], depicted in Fig. S1. The 2D correlation spectra are obtained by Fourier transforming the delays T_1 (coherence time) and $T_3 \equiv t$ (detection time) in the polarization $S_{\text{PE}}(\Omega_3, \Omega_1; T_2) = \int_0^\infty dT_1 \int_0^\infty dT_3 \langle P_{\text{PE}}(T_3, T_2, T_1) \rangle e^{i\Omega_3 T_3 + i\Omega_1 T_1}$.

respective GSB and SE signals, consequently, cross-peaks appear symmetrically below and above the diagonal. Transitions involving CH_2 and CF_2 cores are quartically coupled due to spatial vicinity of the two carbons, i.e., excitations of CH_2 core depends on the occupation number in CF_2 . The associated ESA exhibit a ~ 1.5 eV red-shift (289.6 eV/284.0 eV and 285.6 eV/288.0 eV) or a blue-shift (289.6 eV/294.5 eV and 293.0 eV/291.0 eV) with respect to the corresponding off-diagonal GSB which makes the ESA appear in the 2D spectra. At $g = 2.45$ eV/D, the polariton splitting is reflected in the additional cross peaks between the polariton states and bare molecular states. Similar features are seen in the stronger coupling case shown in Fig. 3 where additional hybrid polariton states

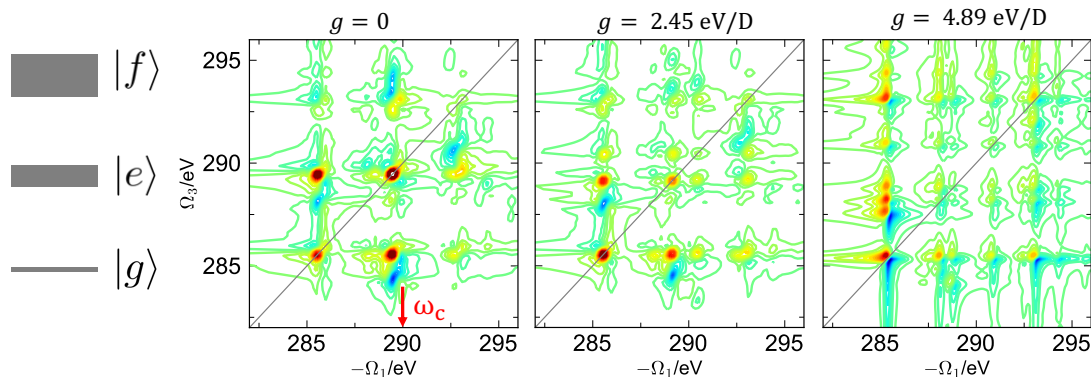


FIG. 3. Level scheme and the 2D photon echo spectra $S_{\text{PE}}(\Omega_3, \Omega_1; T_2 = 0)$ for 1,1-difluoroethylene in an X-ray cavity with $\omega_c = 290$ eV for different coupling strengths as indicated. We use attosecond pulses with central frequency 290 eV and 20 eV bandwidth.

containing excitations from both carbon atoms are created.

We now turn to the double quantum coherence (DQC) signal at $\mathbf{k}_1 + \mathbf{k}_2 - \mathbf{k}_3$ [50–54], represented by the diagrams shown in Fig. S2. The correlations between single- and two-polaritons can be obtained either by Fourier transform of the time-delays T_3 and T_2 at a fixed T_1 , $S_{\text{DQC}}(\Omega_3, \Omega_2; T_1)$ or by Fourier transform of the time-delays T_1 and T_2 at a fixed T_3 , $S_{\text{DQC}}(\Omega_2, \Omega_1; T_3)$. In DQC, the polariton system is in the coherence $|e\rangle\langle g|$ during T_1 , and is then promoted to $|f\rangle\langle g|$ during T_2 . The system can be either $|f\rangle\langle e|$ or $|e\rangle\langle g|$ for the detection time T_3 . The peaks in $S_{\text{DQC}}(\Omega_2, \Omega_1; T_3)$ reveal correlation between ω_{eg} and ω_{fg} . For a harmonic system where $\omega_{fg} = \omega_{eg}$ and for uncorrelated transitions where $\omega_{fg} = \omega_{eg} + \omega_{e'g}$, the DQC signal vanishes as the two contributions to DQC interfere destructively. This makes DQC suitable for resolving anharmonicities and correlated transitions.

The DQC $S_{\text{DQC}}(\Omega_2, \Omega_1; T_3)$ are shown in Fig. 4 for varying cavity coupling strengths. The vertical axis shows the doubly core-excited states $|f\rangle$ that can be reached from $|g\rangle$ through an excited state $|e\rangle$. Prominent contributions at $\Omega_1/\Omega_2 = 285.6$ eV/573.9 eV and 289.5 eV/573.9 eV arise due to the coupling of $\text{CH}_2 \rightarrow \pi^*$ (285.6 eV) and $\text{CF}_2 \rightarrow \pi^*$ (289.5 eV) transitions to the $\text{CH}_2, \text{CF}_2 \Rightarrow \pi^*$ transition [55]. Similarly, peaks at 289.5 eV/584.1 eV and 293.0 eV/584.1 eV arise due to the coupling of $\text{CF}_2 \rightarrow \pi^*$ (289.5 eV) and $\text{CH}_2 \rightarrow \text{Ry}$ (293.0 eV) transitions to the $\text{CH}_2, \text{CF}_2 \Rightarrow \pi^*, \text{Ry}$ transition. In the strong coupling regime, the polariton states manifest as a doublet around $\Omega_1 = 290$ eV. Additional peaks are clearly observed between these single-polariton states and the f -manifold. Core-polaritons also modulate the doubly core-excited states by mixing them with the two-cavity-photon state and single-core-excitation single-cavity-photon state. For example, a noticeable red-shift can be observed for the $\text{CH}_2, \text{CF}_2 \Rightarrow \pi^*$ transition from the slices of the DQC at $\Omega_1 = 285.5$ eV.

The correlations between ω_{fe} and ω_{fg} are revealed in the DQC signal $S_{\text{DQC}}(\Omega_3, \Omega_2; T_1)$ displayed in Fig. 4

(bottom row). States from the doubly excited manifold coupled to the singly excited manifold are characterized through a set of four peaks along Ω_3 for a given Ω_2 value [56]. For example, the quartet of peaks along the $\Omega_2 = 573.9$ eV are associated with two peaks at 285.6 eV and 289.5 eV coinciding with the $\text{CH}_2 \rightarrow \pi^*$ and $\text{CF}_2 \rightarrow \pi^*$ transitions and two red-shifted peaks at 284.4 eV and 288.3 eV corresponding to the $\text{CH}_2 \rightarrow \pi^*$ with CF_2 excited and $\text{CF}_2 \rightarrow \pi^*$ with CH_2 -excited. [57] The 1.2 eV splitting between each pair of corresponds to the value of the quartic coupling between both transitions. Under strong coupling, core-polariton doublets can be observed along Ω_3 due to the ω_{fe} resonances. The splitting does not directly correspond to the polariton resonances because both e and f manifolds are modified by the cavity mode.

Similar information about the correlations of single and double excitations as provided by DQC can be extracted from the two-photon absorption signal, discussed in Sec. S4. This signal does not require coherent X-ray pulses and is thus easier to implement experimentally.

In summary, we have demonstrated how molecular core-excitations can be manipulated by coupling to the vacuum field in an X-ray cavity. Localized excitations from the two carbon atoms in 1,1-difluoroethylene are coherently coupled by the exchange of an X-ray cavity photon creating hybrid delocalized excitations. We identified the spectroscopic signatures of core-polaritons in XANES, two-photon absorption, and multidimensional X-ray spectroscopic signals. XANES directly probes the hybrid core-polariton states with the polariton effects manifested as mode splitting, redistribution of oscillator strength, and line shifts, depending on the cavity frequency and coupling strength. Correlation between polaritonic excitations are revealed by the PE, and information about the two-polariton manifold can be readily extracted from the DQC and two-photon absorption signals. This study shows how to manipulate core-excitations in molecules by strong coupling to a cavity in the X-ray regime. Many interesting phenomena dis-

covered for exciton-polaritons in the optical regime such as long-range transport [35], modified chemical reaction rates [58], enhanced nonlinearity [36] suggest analogous extensions for core-polaritons in the X-ray regime. Relaxation dynamics of core-polaritons is also expected to differ significantly from the bare core-excitations. Collective effects found in Mössbauer resonance in iron including electromagnetically induced transparency and Lamb shift [32, 33] may show up in molecules as well.

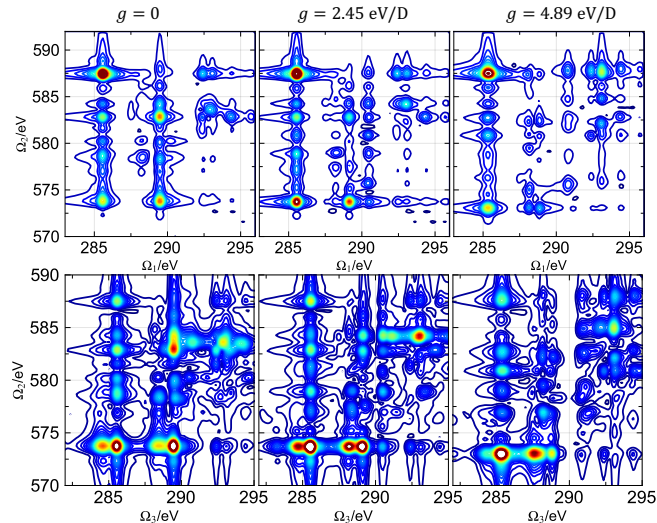


FIG. 4. 2D double quantum coherence spectra $|S_{DQC}(\Omega_2, \Omega_1; T_3)|$ (upper row) and $|S_{DQC}(\Omega_3, \Omega_2; T_1)|$ (lower) in an X-ray cavity with $\omega_c = 290$ eV at different coupling strengths g as indicated. A small time delay 10^{-5} as is used for both T_3 and T_1 to avoid cancellation of the two DQC diagrams.

ACKNOWLEDGMENTS

We thank Dr. Stefano M. Cavaletto for helpful discussions and Dr. Ralf Röhlsberger for valuable feedback. M.G., A.N., F.S., and S.M. acknowledge support from the Chemical Sciences, Geosciences, and Bio-sciences division, Office of Basic Energy Sciences, Office of Science, U.S., Department of Energy, through Award No. DE-SC0019484. B.G. acknowledges the support from the National Science Foundation Grant CHE-1953045.

-
- [1] E. M. Purcell, “Spontaneous emission probabilities at radio frequencies,” *Phys Rev* **69**, 681 (1946).
 - [2] R. H. Dicke, “Coherence in Spontaneous Radiation Processes,” *Phys. Rev.* **93**, 99–110 (1954).
 - [3] Bing Gu and Shaul Mukamel, “Cooperative Conical Intersection Dynamics of Two Pyrazine Molecules in an Optical Cavity,” *J. Phys. Chem. Lett.* **11**, 5555–5562 (2020).
 - [4] Xiaolan Zhong, Thibault Chervy, Lei Zhang, Anoop Thomas, Jino George, Cyriaque Genet, James A. Hutchison, and Thomas W. Ebbesen, “Energy Transfer between Spatially Separated Entangled Molecules,” *Angew. Chem. Int. Ed.* **56**, 9034–9038 (2017).
 - [5] Jino George, Atef Shalabney, James A. Hutchison, Cyriaque Genet, and Thomas W. Ebbesen, “Liquid-Phase Vibrational Strong Coupling,” *J. Phys. Chem. Lett.* **6**, 1027–1031 (2015).
 - [6] A. Shalabney, J. George, J. Hutchison, G. Pupillo, C. Genet, and T. W. Ebbesen, “Coherent coupling of molecular resonators with a microcavity mode,” *Nat. Commun.* **6**, 5981 (2015).
 - [7] Felix Benz, Mikolaj K. Schmidt, Alexander Dreismann, Rohit Chikkaraddy, Yao Zhang, Angela Demetriadou, Cloudy Carnegie, Hamid Ohadi, Bart de Nijs, Ruben Esteban, Javier Aizpurua, and Jeremy J. Baumberg, “Single-molecule optomechanics in “picocavities,”” *Science* **354**, 726–729 (2016).
 - [8] Ki Youl Yang, Dong Yoon Oh, Seung Hoon Lee, Qi-Fan Yang, Xu Yi, Boqiang Shen, Heming Wang, and Kerry Vahala, “Bridging ultrahigh-Q devices and photonic circuits,” *Nat. Photonics* **12**, 297–302 (2018).
 - [9] Thomas W. Ebbesen, “Hybrid Light–Matter States in a Molecular and Material Science Perspective,” *Acc. Chem. Res.* **49**, 2403–2412 (2016).
 - [10] Xiaolan Zhong, Thibault Chervy, Shaojun Wang, Jino George, Anoop Thomas, James A. Hutchison, Eloise Devaux, Cyriaque Genet, and Thomas W. Ebbesen, “Non-Radiative Energy Transfer Mediated by Hybrid Light-Matter States,” *Angew. Chem.* **128**, 6310–6314 (2016).
 - [11] Rohit Chikkaraddy, Bart de Nijs, Felix Benz, Steven J. Barrow, Oren A. Scherman, Edina Rosta, Angela Demetriadou, Peter Fox, Ortwin Hess, and Jeremy J. Baumberg, “Single-molecule strong coupling at room temperature in plasmonic nanocavities,” *Nature* **535**, 127–130

- (2016).
- [12] Bing Gu and Shaul Mukamel, “Manipulating nonadiabatic conical intersection dynamics by optical cavities,” *Chem. Sci.* **11**, 1290–1298 (2020).
 - [13] Markus Kowalewski, Kochise Bennett, Jérémy R. Rouxel, and Shaul Mukamel, “Monitoring Nonadiabatic Electron-Nuclear Dynamics in Molecules by Attosecond Streaking of Photoelectrons,” *Phys. Rev. Lett.* **117**, 043201 (2016).
 - [14] Kochise Bennett, Markus Kowalewski, and Shaul Mukamel, “Novel photochemistry of molecular polaritons in optical cavities,” *Faraday Discuss.* **194**, 259–282 (2016).
 - [15] Christian Schäfer, Michael Ruggenthaler, Heiko Appel, and Angel Rubio, “Modification of excitation and charge transfer in cavity quantum-electrodynamical chemistry,” *Proc. Natl. Acad. Sci. U.S.A.* **116**, 4883–4892 (2019).
 - [16] Javier Galego, Francisco J. Garcia-Vidal, and Johannes Feist, “Cavity-Induced Modifications of Molecular Structure in the Strong-Coupling Regime,” *Phys. Rev. X* **5**, 041022 (2015).
 - [17] Johannes Flick, Michael Ruggenthaler, Heiko Appel, and Angel Rubio, “Atoms and molecules in cavities, from weak to strong coupling in quantum-electrodynamics (QED) chemistry,” *Proc. Natl. Acad. Sci.* **114**, 3026–3034 (2017).
 - [18] Johannes Flick, Nicholas Rivera, and Prineha Narang, “Strong light-matter coupling in quantum chemistry and quantum photonics,” *Nanophotonics* **7**, 1479–1501 (2018).
 - [19] Konstantin E. Dorfman and Shaul Mukamel, “Multidimensional photon correlation spectroscopy of cavity polaritons,” *Proc. Natl. Acad. Sci.* **115**, 1451–1456 (2018).
 - [20] Felipe Herrera and Frank C. Spano, “Absorption and photoluminescence in organic cavity QED,” *Phys. Rev. A* **95**, 053867 (2017), [arXiv:1611.05828](https://arxiv.org/abs/1611.05828).
 - [21] David M. Coles, Niccolo Somaschi, Paolo Michetti, Caspar Clark, Pavlos G. Lagoudakis, Pavlos G. Savvidis, and David G. Lidzey, “Polariton-mediated energy transfer between organic dyes in a strongly coupled optical microcavity,” *Nat. Mater.* **13**, 712–719 (2014).
 - [22] Anton Frisk Kockum, Adam Miranowicz, Simone De Liberato, Salvatore Savasta, and Franco Nori, “Ultrastrong coupling between light and matter,” *Nat. Rev. Phys.* **1**, 19–40 (2019).
 - [23] Parinda Vasa and Christoph Lienau, “Strong Light-Matter Interaction in Quantum Emitter/Metal Hybrid Nanostructures,” *ACS Photonics* **5**, 2–23 (2018).
 - [24] Manuel Hertzog, Mao Wang, Jürgen Mony, and Karl Börjesson, “Strong light-matter interactions: A new direction within chemistry,” *Chem. Soc. Rev.* **48**, 937–961 (2019).
 - [25] Tal Schwartz, James A. Hutchison, Jérémie Léonard, Cyriaque Genet, Stefan Haacke, and Thomas W. Ebbesen, “Polariton Dynamics under Strong Light-Molecule Coupling,” *ChemPhysChem* **14**, 125–131 (2013).
 - [26] Felipe Herrera and Frank C. Spano, “Dark Vibronic Polaritons and the Spectroscopy of Organic Microcavities,” *Phys. Rev. Lett.* **118**, 223601 (2017).
 - [27] Luis A. Martínez-Martínez, Matthew Du, Raphael F. Ribeiro, Stéphane Kéna-Cohen, and Joel Yuen-Zhou, “Polariton-Assisted Singlet Fission in Acene Aggregates,” *J. Phys. Chem. Lett.* **9**, 1951–1957 (2018).
 - [28] Daniele Sanvitto and Stéphane Kéna-Cohen, “The road towards polaritonic devices,” *Nat. Mater.* **15**, 1061–1073 (2016).
 - [29] Bing Gu and Shaul Mukamel, “Manipulating Two-Photon-Absorption of Cavity Polaritons by Entangled Light,” *J. Phys. Chem. Lett.* **11**, 8177–8182 (2020).
 - [30] Arkajit Mandal and Pengfei Huo, “Investigating New Reactivities Enabled by Polariton Photochemistry,” *J. Phys. Chem. Lett.* **10**, 5519–5529 (2019).
 - [31] Ralf Röhlsberger, Jörg Evers, and Sharon Schwartz, “Quantum and Nonlinear Optics with Hard X-Rays,” in *Synchrotron Light Sources and Free-Electron Lasers*, edited by Eberhard J. Jaeschke, Shaikat Khan, Jochen R. Schneider, and Jerome B. Hastings (Springer International Publishing, Cham, 2020) pp. 1399–1431.
 - [32] R. Röhlsberger, K. Schlage, B. Sahoo, S. Couet, and R. Ruffer, “Collective Lamb Shift in Single-Photon Superradiance,” *Science* **328**, 1248–1251 (2010).
 - [33] Ralf Röhlsberger, Hans-Christian Wille, Kai Schlage, and Balaram Sahoo, “Electromagnetically induced transparency with resonant nuclei in a cavity,” *Nature* **482**, 199–203 (2012).
 - [34] Johann Haber, Jakob Gollwitzer, Sonia Francoual, Martin Tolkiehn, Jörg Stempfer, and Ralf Röhlsberger, “Spectral Control of an X-Ray L-Edge Transition via a Thin-Film Cavity,” *Phys. Rev. Lett.* **122**, 123608 (2019).
 - [35] Georgi Gary Rozenman, Katherine Akulov, Adina Golombek, and Tal Schwartz, “Long-Range Transport of Organic Exciton-Polaritons Revealed by Ultrafast Microscopy,” *ACS Photonics* **5**, 105–110 (2018).
 - [36] Thibault Chervy, Jialiang Xu, Yulong Duan, Chunliang Wang, Loïc Mager, Maurice Frerejean, Joris A. W. Münninghoff, Paul Tinnemans, James A. Hutchison, Cyriaque Genet, Alan E. Rowan, Theo Rasing, and Thomas W. Ebbesen, “High-Efficiency Second-Harmonic Generation from Hybrid Light-Matter States,” *Nano Lett.* **16**, 7352–7356 (2016).
 - [37] Shaul Mukamel, *Principles of Nonlinear Optical Spectroscopy* (Oxford University Press, 1995).
 - [38] Bo Xiang, Raphael F. Ribeiro, Adam D. Dunkelberger, Jiaxi Wang, Yingmin Li, Blake S. Simpkins, Jeffrey C. Owrutsky, Joel Yuen-Zhou, and Wei Xiong, “Two-dimensional infrared spectroscopy of vibrational polaritons,” *Proc Natl Acad Sci USA* **115**, 4845–4850 (2018).
 - [39] C. Pellegrini, A. Marinelli, and S. Reiche, “The physics of x-ray free-electron lasers,” *Rev. Mod. Phys.* **88**, 015006 (2016).
 - [40] S. Mukamel, D. Healion, Y. Zhang, and J. D. Biggs, “Multidimensional attosecond resonant X-ray spectroscopy of molecules: Lessons from the optical regime,” *Annu Rev Phys Chem* **64**, 101–127 (2013).
 - [41] Satoshi Tanaka and Shaul Mukamel, “X-ray four-wave mixing in molecules,” *J. Chem. Phys.* **116**, 1877–1891 (2002).
 - [42] Jason D. Biggs, Yu Zhang, Daniel Healion, and Shaul Mukamel, “Two-dimensional stimulated resonance Raman spectroscopy of molecules with broadband x-ray pulses,” *The Journal of Chemical Physics* **136**, 174117 (2012).
 - [43] Artur Nenov, Francesco Segatta, Adam Bruner, Shaul Mukamel, and Marco Garavelli, “X-ray linear and nonlinear spectroscopy of the ESCA molecule,” *J. Chem. Phys.* **151**, 114110 (2019).
 - [44] Courtney A. DelPo, Bryan Kudisch, Kyu Hyung Park, Saeed-Uz-Zaman Khan, Francesca Fassioli, Daniele

- Fausti, Barry P. Rand, and Gregory D. Scholes, "Polariton Transitions in Femtosecond Transient Absorption Studies of Ultrastrong Light-Molecule Coupling," *J. Phys. Chem. Lett.* **11**, 2667–2674 (2020).
- [45] See Supplemental Material for details of the electronic structure and spectroscopic computations, which includes Refs. [59–72].
- [46] R. McLaren, S. A. C. Clark, I. Ishii, and A. P. Hitchcock, "Absolute oscillator strengths from K-shell electron-energy-loss spectra of the fluoroethenes and 1,3-perfluorobutadiene," *Phys. Rev. A* **36**, 1683–1701 (1987).
- [47] S. Schütz, J. Schachenmayer, D. Hagenmüller, G. K. Brennen, T. Volz, V. Sandoghdar, T. W. Ebbesen, C. Genes, and G. Pupillo, "Ensemble-Induced Strong Light-Matter Coupling of a Single Quantum Emitter," *Phys. Rev. Lett.* **124**, 113602 (2020).
- [48] Ashok Muthukrishnan, Girish S. Agarwal, and Marlan O. Scully, "Inducing Disallowed Two-Atom Transitions with Temporally Entangled Photons," *Phys. Rev. Lett.* **93**, 093002 (2004).
- [49] Marten Richter and Shaul Mukamel, "Collective two-particle resonances induced by photon entanglement," *Phys. Rev. A* **83**, 063805 (2011).
- [50] Marten Richter and Shaul Mukamel, "Ultrafast double-quantum-coherence spectroscopy of excitons with entangled photons," *Phys. Rev. A* **82**, 013820 (2010).
- [51] Igor V. Schweigert and Shaul Mukamel, "Double-quantum-coherence attosecond x-ray spectroscopy of spatially separated, spectrally overlapping core-electron transitions," *Phys. Rev. A* **78**, 052509 (2008).
- [52] Jeongho Kim, Shaul Mukamel, and Gregory D. Scholes, "Two-Dimensional Electronic Double-Quantum Coherence Spectroscopy," *Acc. Chem. Res.* **42**, 1375–1384 (2009).
- [53] Xingcan Dai, Marten Richter, Hebin Li, Alan D. Bristow, Cyril Falvo, Shaul Mukamel, and Steven T. Cundiff, "Two-Dimensional Double-Quantum Spectra Reveal Collective Resonances in an Atomic Vapor," *Phys. Rev. Lett.* **108**, 193201 (2012).
- [54] Darius Abramavicius, Alexandra Nemeth, Franz Milota, Jaroslaw Sperling, Shaul Mukamel, and Harald F. Kauffmann, "Weak Exciton Scattering in Molecular Nanotubes Revealed by Double-Quantum Two-Dimensional Electronic Spectroscopy," *Phys. Rev. Lett.* **108**, 067401 (2012).
- [55] Here \Rightarrow indicates a double excitation.
- [56] Artur Nenov, Ivan Rivalta, Shaul Mukamel, and Marco Garavelli, "Bidimensional electronic spectroscopy on indole in gas phase and in water from first principles," *Comput. Theor. Chem Excited States: From Isolated Molecules to Complex Environments*, **1040-1041**, 295–303 (2014).
- [57] Here, the brackets indicate that the core-excitation occurs in the presence of a core-excited carbon.
- [58] James A. Hutchison, Tal Schwartz, Cyriaque Genet, Eloïse Devaux, and Thomas W. Ebbesen, "Modifying Chemical Landscapes by Coupling to Vacuum Fields," *Angew. Chem. Int. Ed.* **51**, 1592–1596 (2012).
- [59] Niclas Forsberg and Per-Ake Malmqvist, "Multiconfiguration perturbation theory with imaginary level shift," *Chem. Phys. Lett.* **274**, 196–204 (1997).
- [60] Per-Ake Malmqvist, Alistair Rendell, and Björn O. Roos, "The restricted active space self-consistent-field method, implemented with a split graph unitary group approach," *J. Phys. Chem.* **94**, 5477–5482 (1990).
- [61] Marcus Lundberg and Mickaël G. Delcey, *Transition Metals in Coordination Environments*, edited by Ewa Broclawik, Tomasz Borowski, and Mariusz Radoń (Springer International Publishing, 2019) Chap. Multiconfigurational Approach to X-ray Spectroscopy of Transition Metal Complexes.
- [62] Kerstin Andersson, Per-Ake Malmqvist, Bjoern O. Roos, Andrzej J. Sadlej, and Krzysztof Wolinski, "Second-order perturbation theory with a CASSCF reference function," *J. Phys. Chem.* **94**, 5483–5488 (1990).
- [63] Vicenta Sauri, Luis Serrano-Andrés, Abdul R. M. Shahi, Laura Gagliardi, Steven Vancoillie, and Kristine Pierloot, "Multiconfigurational second-order perturbation theory restricted active space (RASPT2) method for electronic excited states: A benchmark study." *J. Chem. Theory Comput.* **7**, 153 (2011).
- [64] Daniel Roca-Sanjuán, Francesco Aquilante, and Roland Lindh, "Multiconfiguration second-order perturbation theory approach to strong electron correlation in chemistry and photochemistry," *Wiley Interdiscip. Rev. Comput. Mol. Sci.* **2**, 585–603 (2011).
- [65] Giovanni Ghigo, Björn O. Roos, and Per-Ake Malmqvist, "A modified definition of the zeroth-order Hamiltonian in multiconfigurational perturbation theory (CASPT2)," *Chem. Phys. Lett.* **396**, 142–149 (2004).
- [66] J. Patrick Zobel, Juan J. Nogueira, and Leticia González, "The IPEA dilemma in CASPT2," *Chem. Sci.* **8**, 1482–1499 (2017).
- [67] Thomas Bondo Pedersen, Francesco Aquilante, and Roland Lindh, "Density fitting with auxiliary basis sets from Cholesky decompositions," *Theor. Chem. Acc.* **124**, 1–10 (2009).
- [68] Markus Kowalewski, Benjamin P. Fingerhut, Konstantin E. Dorfman, Kochise Bennett, and Shaul Mukamel, "Simulating Coherent Multidimensional Spectroscopy of Nonadiabatic Molecular Processes: From the Infrared to the X-ray Regime," *Chem. Rev.* **117**, 12165–12226 (2017).
- [69] Björn O. Roos, Valera Veryazov, and Per-Olof Widmark, "Relativistic atomic natural orbital type basis sets for the alkaline and alkaline-earth atoms applied to the ground-state potentials for the corresponding dimers," *Theor. Chem. Acc.* **111**, 345–351 (2004).
- [70] Ignacio Fdez. Galván, Morgane Vacher, Ali Alavi, Celestino Angeli, Francesco Aquilante, Jochen Autschbach, Jie J. Bao, Sergey I. Bokarev, Nikolay A. Bogdanov, Rebecca K. Carlson, Liviu F. Chibotaru, Joel Creutzberg, Nike Dattani, Mickaël G. Delcey, Sijia S. Dong, Andreas Dreuw, Leon Freitag, Luis Manuel Frutos, Laura Gagliardi, Frédéric Gendron, Angelo Giussani, Leticia González, Gilbert Grell, Meiyuan Guo, Chad E. Hoyer, Marcus Johansson, Sebastian Keller, Stefan Knecht, Goran Kovačević, Erik Källman, Giovanni Li Manni, Marcus Lundberg, Yingjin Ma, Sebastian Mai, João Pedro Malhado, Per Ake Malmqvist, Philipp Marquetand, Stefanie A. Mewes, Jesper Norell, Massimo Olivucci, Markus Oppel, Quan Manh Phung, Kristine Pierloot, Felix Plasser, Markus Reiher, Andrew M. Sand, Igor Schapiro, Prachi Sharma, Christopher J. Stein, Lasse Kragh Sørensen, Donald G. Truhlar, Mihkel Ugandi, Liviu Ungur, Alessio Valentini, Steven Vancoillie, Valera Veryazov, Oskar Weser, Tomasz A. Wesolowski, Per-Olof Widmark, Sebastian Wouters,

- Alexander Zech, J. Patrick Zobel, and Roland Lindh, “OpenMolcas: From Source Code to Insight,” *J. Chem. Theory Comput.* **15**, 5925–5964 (2019).
- [71] Francesco Aquilante, Jochen Autschbach, Alberto Baiardi, Stefano Battaglia, Veniamin A. Borin, Liviu F. Chibotaru, Irene Conti, Luca De Vico, Mickaël Delcey, Ignacio Fdez. Galván, Nicolas Ferré, Leon Freitag, Marco Garavelli, Xuejun Gong, Stefan Knecht, Ernst D. Larsson, Roland Lindh, Marcus Lundberg, Per rAke Malmqvist, Artur Nenov, Jesper Norell, Michael Odellius, Massimo Olivucci, Thomas B. Pedersen, Laura Pedraza-González, Quan M. Phung, Kristine Pierloot, Markus Reiher, Igor Schapiro, Javier Segarra-Martí, Francesco Segatta, Luis Seijo, Saumik Sen, Dumitru-Claudiu Sergentu, Christopher J. Stein, Liviu Ungur, Morgane Vacher, Alessio Valentini, and Valera Veryazov, “Modern quantum chemistry with [Open]Molcas,” *J. Chem. Phys.* **152**, 214117 (2020).
- [72] Konstantin E. Dorfman and Shaul Mukamel, “Nonlinear spectroscopy with time- and frequency-gated photon counting: A superoperator diagrammatic approach,” *Phys. Rev. A* **86**, 013810 (2012).